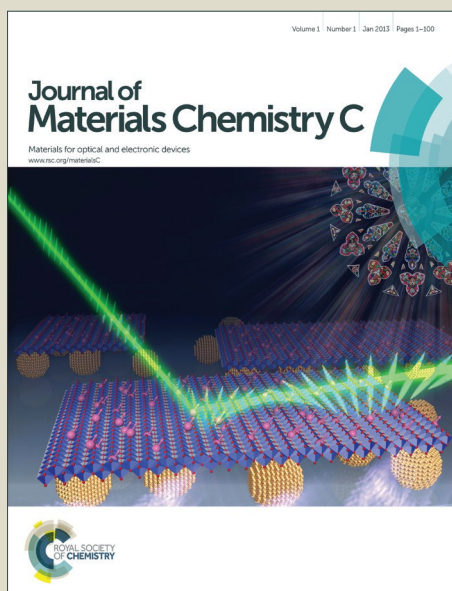


Journal of Materials Chemistry C

Accepted Manuscript



This article can be cited before page numbers have been issued, to do this please use: E. P. Pozhidaev,, V. V. Vashchenko, V. V. Mikhailenko, A. I. Krivoshey, V. A. Barbashov, L. Shi, A. K. Srivastava, V. Chigrinov and H. S. Kwok, *J. Mater. Chem. C*, 2016, DOI: 10.1039/C6TC04087J.



This is an *Accepted Manuscript*, which has been through the Royal Society of Chemistry peer review process and has been accepted for publication.

Accepted Manuscripts are published online shortly after acceptance, before technical editing, formatting and proof reading. Using this free service, authors can make their results available to the community, in citable form, before we publish the edited article. We will replace this *Accepted Manuscript* with the edited and formatted *Advance Article* as soon as it is available.

You can find more information about *Accepted Manuscripts* in the [Information for Authors](#).

Please note that technical editing may introduce minor changes to the text and/or graphics, which may alter content. The journal's standard [Terms & Conditions](#) and the [Ethical guidelines](#) still apply. In no event shall the Royal Society of Chemistry be held responsible for any errors or omissions in this *Accepted Manuscript* or any consequences arising from the use of any information it contains.



Journal Name

ARTICLE

Ultrashort helix pitch antiferroelectric liquid crystals based on chiral esters of terphenyldicarboxylic acid

E.P. Pozhidaev,^{a,b} V.V. Vashchenko,^{a,c} V. V. Mikhailenko,^c A.I. Krivoshey,^c
V.A. Barbashov,^b L. Shi,^a A.K. Srivastava,^{*a} V.G. Chigrinov,^a and H.S. Kwok^a

Received 00th January 20xx,
Accepted 00th January 20xx

DOI: 10.1039/x0xx00000x

www.rsc.org/

Antiferroelectric liquid crystals (AFLCs) with nanoscale helix pitch (<100 nm) were revealed in a composition containing achiral smectic-C biphenylpyrimidines and two non-mesogenic chiral dopants: p-terphenyldicarboxylates of chiral (2S)-1,1,1-trifluorooctane-2-ol and (S,S)-1,1,1-trifluorooctan-2-yl 2-hydroxypropanoate. The prepared multicomponent AFLCs exhibit two electro-optical effects, which are interrelated with the chemical structures of the mixtures components. First effect is hysteresis free under a special voltage waveform U-shaped switching, which exhibits the electro-optical response similar to nematic liquid crystals (NLCs) but around 1 - 2 orders of magnitude faster. Second, deformed helix antiferroelectric liquid crystal (DHAFLC) effect has been investigated. The observed temperature independence of the electro-optical parameters, in a certain temperature range, combined with fast U-shape response or with DHAFLC, adds a great value for applications.

Introduction

AFLCs are innovative electro-optical materials with great potential in various display and photonic applications.¹⁻⁵ In spite of AFLCs were a long ago employed to develop prototypes of displays,⁶⁻⁸ and great success in AFLC material science for subsequent years,^{1,9-14} displays based on such materials are still far from being commercial.^{1,14} Main inherent drawbacks hampering AFLCs commercial application are the sensitivity of the uniform alignment to mechanical shock, very pronounced double W-shaped hysteresis loop, and the dark state problem (or simply insufficient alignment quality of AFLC display cells).^{1,15} Unfortunately, even modern AFLC materials are not free from all of these disadvantages. Thus, in the polymer-stabilized AFLC^{3,16,17} including those based on bent-core molecules^{11,18} are insensitive to mechanical shock and hysteresis free¹¹. However, the contrast ratio of the electro-optical modulation is rather low.³ In

contrary, the so-called orthoconic AFLCs,^{5,12,13,19} provide excellent optical quality of AFLCs display cells due to 45° tilt angle, but their antiferroelectric C_A* phase at room temperature is rather slow in electro-optical response^{4,8,20-22}. Compensation of the hysteresis in electro-optical response can be achieved in this case only by using a very intricate driving voltage waveform¹⁴ or asymmetric switching due to different anchoring surfaces,²³ which is very difficult to implement in display technology.

It is also worth to note, that most of known AFLC devices have been targeted for using in SSFLC mode where rather long helix pitch is preferable, typically from few μm.^{1,2,4,5} But typical helix pitch values of most of AFLC materials are around of 1 μm,⁴ and special efforts were applied to increase the pitch in order to harmonize it with LC cell thickness. On the contrary, the mentioned pitch values are too large for effective applications using short-pitch electrooptical modes, e.g. as deformed helix ferroelectric (DHF) effect in SmC* phase.²⁴ Hence, application potential of ultrashort helix pitch AFLCs has not been considered so far.

Here we report on design and synthesis of new chiral trifluoromethylated esters of terphenyl-dicarboxylic acid which are in mixtures with biphenylpyrimidine host allowed to elaborate ultrashort AFLC materials exhibiting DHF and hysteresis free U-shaped electro-optical switching.

^a State Key Laboratory on Advanced Displays and Optoelectronics Technologies, Department of Electronic and Computer Engineering, The Hong Kong University of Science and Technology, Clear Water Bay, Kowloon, Hong Kong, China.

*Email: Abhishek_Srivastava_lu@yahoo.co.in

^b P.N. Lebedev Physics Institute of the Russian Academy of Sciences, Leninskiy pr. 53, Moscow 119991, Russia.

^c State Scientific Institution "Institute for Single Crystals", Nauki Ave., 60, Kharkov 61001, Ukraine.

† Electronic Supplementary Information (ESI) available: full description of experimental procedures, data of materials and instrument specification are given in Supplementary Information. See DOI: 10.1039/x0xx00000x

Materials and methods

Structural design of chiral dopants

Structural requirements to chemical compounds exhibiting AFLC ordering hitherto are formulated only in very general terms and mainly with respect to individual mesogens (Fig. 1).^{1,2,4,25,26} Thus, anticlinic phases are often formed by bent-core or by so-called bi-mesogens (Figs. 1a and 1b).^{11,18,27} However, because of their high viscosity these types of structures will not be further considered.

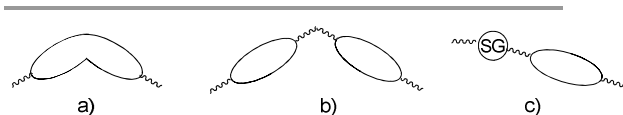
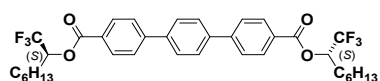


Fig. 1 Schematic drawing of molecule types prone to formation of anticlinic packing.

One of the general structure requirements for single-core LC substances (Fig. 1c) which are prone to anticlinic packing is presence at least three rings in the central core.^{2,26,28} Besides, the probability of formation of anticlinic smectic arrangement typically increases with enhancement of inter-layer interactions. It can be achieved by means of modification of the terminal tails with specifically interacting groups, often highly polar group (SG), which is separated from the core with several methylene units. Among these "specific groups", ether or ester function,^{10,12,13,29} siloxanes,^{9,28,30} partially fluorinated alkyls^{19,31,32} and trifluoromethyl unit^{12,13,24,33} often occurs.

In our structural design, the well-known chiral diesters of *p*-terphenyl dicarboxylic acid³⁴ have been chosen as a basic motif. In particular, we exploited recently described (*S,S*)-*bis*-(1,1,1-trifluorooct-2-yl)-4,4''-terphenyl dicarboxylate (**S-FOTDA-6**):³⁵



which is non-mesogenic itself but induces chiral smectic *C** phase in its mixtures with two or three-ring achiral SmC hosts with the spontaneous polarization P_s 110–160 nC/cm² and sub-wavelength helix pitch p_0 estimated \approx 150–220 nm.^{35–38}

Although, as it was mentioned above that the trifluoromethyl group in a terminal chain often promotes formation of anticlinic packing, we have not observed antiferroelectric phase in any of the LC mixtures containing individual dopant **S-FOTDA-6**.^{36–38}

We suppose that in combination with high helical twisting power (HTP), a very high spontaneous polarization is an additional factor for the appearance of the anticlinic packing because of minimization of the electrostatic energy excess. Following this hypothesis,

we envisaged further increasing of the P_s in LC mixtures. Because of the natural concentration limit for the compatibility of an individual dopant with the SmC host, the required CDs content can be raised in the mixtures of several chiral compounds of the same sign of spontaneous polarization as well as helical twisting.

Thus, it is reasonable to choose **S-FOTDA** as the first chiral dopant. With the additional dopant, we have attempted to increase P_s by combining the CF₃ function with chiral *S*-lactate unit, which is also often deployed in the structure of the FLC dopants particularly in the *S*-lactate esters of terphenyl-dicarboxylic acid (**LACT**)^{37,39,40}. The designed chemical formula of the new dopant is given below (see Fig. 2). The proposed structures of the new dopants, also follows the general tendency of the anticlinic packing appearance (see above), due to a shift of the fluorinated substituent away from the rigid terphenyl core, thereby closing them to the type **c** (see Fig. 1).

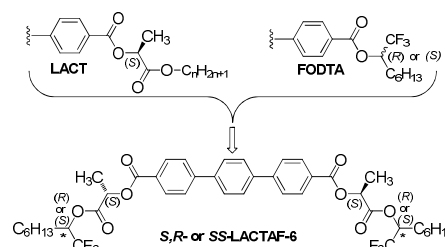


Fig. 2 The design of new chiral dopant of **LACTAF-6** series.

It is worth to point that the presence of two chiral centers at each wing of a **LACTAF** molecules results in appearance as four possible diastereomers combined in two mirror pairs (*S,S* and *R,R*) and (*R,S* and *S,R*). Combining the natural *S*-lactate with synthetic *S*- or *R*-trifluoromethylalkanols the representative diastereomers of each pair mentioned above have been prepared and studied (**S,R-LACTAF-6**, **S,S-LACTAF-6**).

As non-chiral LC host, the mixture (**M1**) of two known biphenylpyrimidines⁴¹ has been chosen as a wide-range SmC non-chiral host (see Fig. 3):

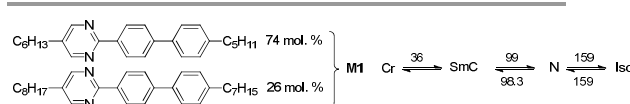


Fig. 3 Chemical structures of components of non-chiral SmC host and its phase transitions (temperatures are given in °C).

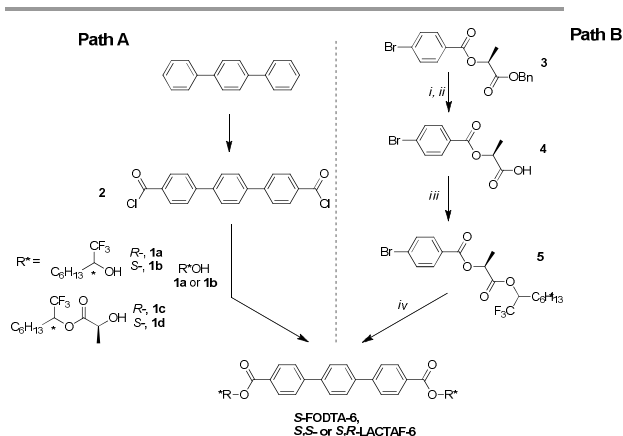
Synthesis

Chiral trifluoromethylalkanols (**1a**, **1b**, see Scheme 1) were obtained in a high enantiomeric purity using enzymatic kinetic resolution,^{42,43} that we have modified recently⁴⁴. Synthesis of **S-FOTDA-6** was carried out as it

was described for its *R*-analogue³⁶ from the terphenyl-dicarboxylic acid chloride (**2**, Scheme 1, path A).

However, the diastereomeric compounds **S,R**- or **S,S**-LACTAF-6 cannot be synthesized by path A because we had failed in obtaining required intermediate trifluoromethyl lactate **1c** or **1d** (see Supplementary Information). Therefore, we have proposed another strategy where terphenyl core is assembled at the latest step *via* cross-coupling of a bromo-benzoic acid derivative **3** with 1,4-phenyldiboric acid (Scheme 1, Path B).

Briefly, *p*-bromobenzoic acid was esterified with *S*-benzyl lactate under carbodiimide methodology⁴⁵ to give chiral ester **3**. It's following catalytic hydrogenolysis does not occur in ethyl acetate according to HPLC. Attempts to run the reaction in methanol lead mainly to transesterification of the ester **3** with methanol and accompanied with the reduction of aromatic bromine atom (according to GC-MS). Taking *tert*-butyl alcohol as a solvent allows suppressing the transesterification however the reaction mixture still quickly degrades which results in a complex mixture where target acid **4** is found by HPLC only as one of the major products. Assuming acid-catalyzed nature of side processes, we have used an excess of pyridine in order to buffer the reaction mixture.



Scheme 1 Synthesis of the diastereomeric **S,R**- and **S,S**-LACTAF-6. *Reagents and conditions:* *i.* (*S*)-benzyl lactate, DCC, DMAP, CH₂Cl₂, 0°C→rt; *ii.* H₂ (1 atm.), Pd/C, pyridine, *tert*-butyl alcohol; *iii.* (*R*)- or (*S*)-1,1,1-trifluoroctan-2-ol, DCC, DMAP, CH₂Cl₂, 0°C→rt; *iv.* 1,4-phenyldiboric acid, PdCl₂dppf (cat.), NaHCO₃ (aq.), SDS, *n*-butanol, toluene, Δ.

Thus, target chiral acid **4** was obtained in satisfactory yield (65%) and purity (98% according to HPLC; see Supplementary Information). The acid **4** was esterified with the corresponding enantiomeric alcohols **1a** and **1b** to give diastereomeric esters **SR-4**, **SS-4**. The esters **SR-4**, **SS-4** reacted with 1,4-phenyldiboric acid by palladium-catalyzed Suzuki cross-coupling reaction in a micro-emulsion⁴⁶ to give

target **S,R**-LACTAF-6 and **S,S**-LACTAF-6. A full description of experimental procedures, data of materials and instrument specification are given in Supplementary Information.

Measurements

The phase transitions temperatures were determined using polarization microscopy (POM), differential scanning calorimetry (DSC), dielectric and electro-optical measurements. Experimental cells were placed into a specially designed heat chamber; the accuracy of temperature measurement is ±0.1°C.

The electro-optical measurements of the tilt angle $\theta(T)$, deflection angle $\Psi(E)$ of the helix principal axis in the presence of the electric field, response time $\tau_{0.1-0.9}(T,E)$ and light transmittance $T_{LT}(T,E)$ were studied in an automatic regime. The basic element of the experimental setup is computer data acquisition (DAQ) board NIPCI 6251 from National Instruments. A detailed description of the electro-optical measurements methods is contained in our previous works.^{36,37,47}

Measurements of the dependencies $T_{LT}(E)$ and $\Psi(E)$ allow to evaluate an effective birefringence $\Delta n_{eff}(E)$ in electric field through the formula,⁴⁸ which is valid for FLCs and AFLCs with sub-wavelength helix pitch:

$$T_{LT}(E) = \sin^2 2[\Psi(E) + \beta] \sin^2 \frac{\pi \Delta n_{eff}(E) d_{AFLC}}{\lambda} \quad (1)$$

where λ is wavelength, d_{AFLC} is the AFLC layer thickness, and β is the angle between the rubbing direction and the plane of polarization of the incident light.

The rotational viscosity γ_{ϕ} was measured by an electro-optic method that is described in details.^{49,50}

Antiferroelectric smectic C_{A*}, ferroelectric and smectics C* phases were identified by the characteristic hysteresis loops in polarization P of planar aligned LC cells on the application of triangular voltage waveform. The spontaneous polarization for different LCs has been measured by the polarization reversal current method,⁵¹ which excludes components of the electric polarization related with the polarizability of molecules rather than with supramolecular structure. The dielectric susceptibility $\chi_G(E)$ of the AFLC helical structure (known as Goldstone mode) has been extracted from measured $P(E)$ dependence through the general definition (2):

$$\chi_G(E) = \frac{1}{\epsilon_0} \left. \frac{\partial P(E)}{\partial E} \right|_{T, \rho = const} \quad (2),$$

where ϵ_0 is permittivity of vacuum, T is temperature, ρ is the density of a test substance.

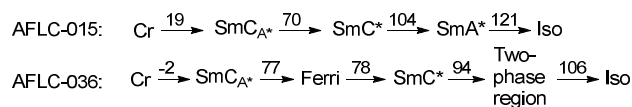
Homeotropic alignment of LC in cells of 20 μm thickness is assured by coating a thin layer of chromo

stearylchloride, 5% wt/wt solution in isopropanol, onto the substrate.³⁶ The cells with homogeneous alignment and thickness 1.5 - 1.7 μm were fabricated with rubbed nylon-6 layers.

Results and discussion

Both diastereomers of **LACTAF-6** and **S-FOTDA-6** are non-mesogenic, however, they are readily soluble in **M1** and even have a stabilizing effect on smectic phases at low concentrations; the destruction of smectic ordering is pronounced over 20-25 mol. % concentration of CD. Nevertheless, due to a wide SmC temperature range of **M1**, it is possible to reach CD concentrations up to 36 mol. % retaining SmC* phase up to 90 °C (see phase diagram in Supplementary Information).

A preliminary study of ferroelectric properties for the new CDs of **LACTAF** series shows that only *S,R*-diastereomer have the same sign of P_s and helix handedness as **S-FODTA-6**, whereas *S,S*-**LACTAF-6** exhibits opposite signs of these parameters. The doping of **M1** with 21 mol % of *S,R*-**LACTAF-6** results in an induction of ferroelectric LC phase which is characterized by the sub-wavelength pitch, and exceptional hysteresis free electro-optical switching with response time $\leq 50\mu\text{s}$. Moreover, we did not observe any anticlinic phases for the **LACTAF** based mixtures. Therefore, because of the favourable optoelectronic performance of **SR-LACTAF-6**, we decided to study it as a second counterpart together with **S-FOTDA-6** in the molar ratios of 4:3 (that is close to their eutectic) as binary chiral dopants (CDs) for doping in the host **M1**. This binary chiral composition is also readily soluble in **M1** without any crucial suppression of the mesophase for the concentration up to 36 mol. %. The most remarkable feature of the four-component mixtures is an unexpected induction of AFLC ordering for the concentration ≥ 15.0 mol % of binary CD. Thus, appearance of anticlinic packing for this mixture (**AFLC-015**) is observed below 70 °C and for 36 mol % concentrated mixtures (**AFLC-036**) – below 76.5 °C; the phase sequences are given below:



Anticlinic packing of **AFLC-036** in the temperature range 0 – 77 °C unambiguously follows typical $P(E)$ hysteresis loop (Fig. 4), and the saturation levels of the loop correspond to the spontaneous polarization P_s value: $P_s \cong 400 \text{ nC/cm}^2$. However, in the case of **AFLC-036**, in contrast to the typical hysteresis loops of AFLCs, no pronounced threshold is observed. It can be

distinguishable only from the plot of the dielectric susceptibility, $\chi_G(E)$, versus the electric field, see left top insertion to Fig. 4. Maximum of the $\chi_G(E)$ dependence corresponds to a critical electric field (E_c) of the AFLC helix unwinding, which is a good criterion for quantitative AFLC characterization in the electric field.

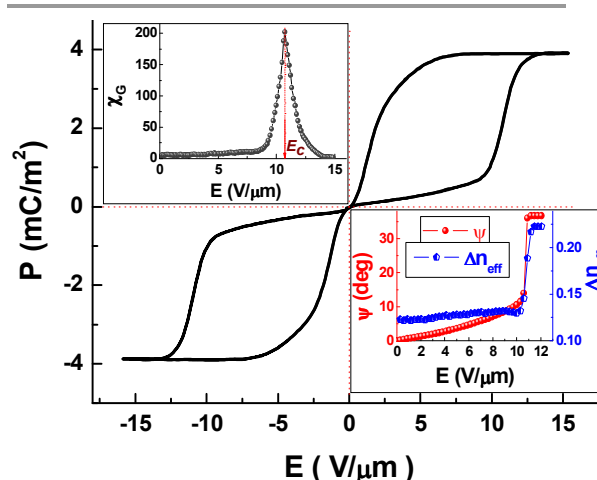


Fig. 4 (Colour online). Hysteresis of current polarization under applied triangular voltage with frequency $f = 1 \text{ Hz}$. Insertion right bottom: deflection angle $\Psi(E)$ of the principal axis and effective birefringence $\Delta n_{\text{eff}}(E)$ at $\lambda = 632.8 \text{ nm}$ of the **AFLC-036** helical structure. Insertion left top: dielectric susceptibility that corresponds to growing branch of the loop at $E > 0$. All results have been obtained in 1.7 μm electro-optical cell at temperature $T = 24^\circ\text{C}$.

The transition in the electric field between the helical and spatially homogeneous structures for a AFLC occurs near E_c , where one can also see the abrupt change of the effective birefringence $\Delta n_{\text{eff}}(E)$ value (approximately 1.7 times) and principle axis deflection angle $\Psi(E)$ of the AFLC helical structure in electric field (right insertion to Fig. 4). Obviously, the saturation level of $\Psi(E)$ corresponds to the tilt angle θ of molecules in smectic layers.

On the other hand, the P_s of **AFLC-036** decreases monotonically at a higher temperature in the temperature range $0^\circ\text{C} \leq T \leq 95^\circ\text{C}$ (Fig. 5). The sharp ramp of P_s value within minus 10°C to 0°C corresponds to melting of the **AFLC-036**.

The synthesized CDs possess very high twisting power, and therefore, the measurement of the pitch by means of selective reflection becomes a non-trivial problem. The selective reflection bands, with the decreasing temperature, move in the UV range, and thereafter, disappear from the spectrum. Therefore, to estimate the pitch of the highly doped mixture we are forced to resort on the electro-optical measurements. Thus in the process, first we have measured the helix pitch p_0 value for the mixture **AFLC-015**, i.e. with 15.5% CD concentration, by the selective reflection (insert to Fig. 5).

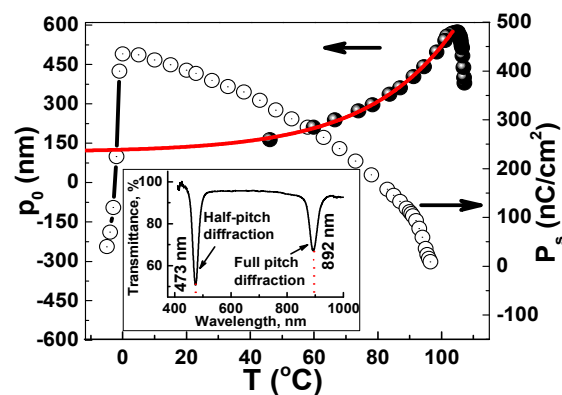


Fig. 5. Temperature dependence of the spontaneous polarization P_s of the **AFLC-036** (open circles) measured at heating from preliminary obtained solid crystal state starting from -10°C . The temperature dependence of the pitch for **AFLC-015** is represented by the black circles. The solid line shows extrapolation of the measured p_0 values to the low-temperature region. The insertion shows the selective light diffraction for the mixture of **AFLC-015** of binary chiral dopant in **M1** host at oblique light incidence ($\xi = 70^\circ$) taken at 78.1°C as an example.

The temperature dependence of the pitch for this mixture has been shown in Fig. 5, at the room temperature the pitch is around 140nm . Both the full and the half pitch peaks were observed for the inclined cell, which is also described the previously.⁵²⁻⁵⁴ On the other hand, the electro-optical relaxation time (τ_{off}) for small deformation of the helix can be given by

$$\tau_{off} \cong \gamma_\phi / K_\phi q_0^2 \quad (3)$$

Here K_ϕ is the elastic constant of the helix twisting and q_0 is the wave vector of the helix. Thus, by comparing the two τ_{off} according to (3) for the two mixtures with known γ_ϕ we can estimate the value of the pitch for the highly concentrated mixtures. In ref. 55, it is experimentally established that the K_ϕ is almost independent on the CD concentration. Thus, we assume that the change in the K_ϕ for the **AFLC-015** and **AFLC-036**, is insignificant. Whereas, as expected, the γ_ϕ decreases at higher temperatures. At the temperature of 40°C , the γ_ϕ of the **AFLC-036** is $\sim 0.2\text{ Pa}\cdot\text{s}$ (Fig. 6a), however, for the **AFLC-015**, in the same ambient and experimental conditions, the $\gamma_\phi \sim 0.095\text{ Pa}\cdot\text{s}$, the smaller CD concentration in **AFLC-015** is responsible for the lower viscosity. Furthermore, the τ_{OFF} of the **AFLC-036** and **AFLC-015** are 20 and $150\mu\text{s}$ respectively. Thus, on comparing the pitch of **AFLC-015** at 40°C ($p_0 = 160\text{nm}$, see Fig. 5 for a clarification) with the pitch of **AFLC-036**, in the light of eq. (3), the pitch for the **AFLC-036** turns out to be $\sim 36\text{nm}$ at 40°C .

Additionally, the **AFLC-036** is characterized by a weak temperature dependence of the tilt angle $\theta(T)$ for the temperature below 60°C (Fig. 6a), which is favourable for applications in various display and photonic devices. Furthermore, a satisfactory alignment quality of the **AFLC-036** (see insertion to Fig.

6c) means that there are no reasonable dark state problems¹⁵ of this AFLC with nanoscale helix pitch.

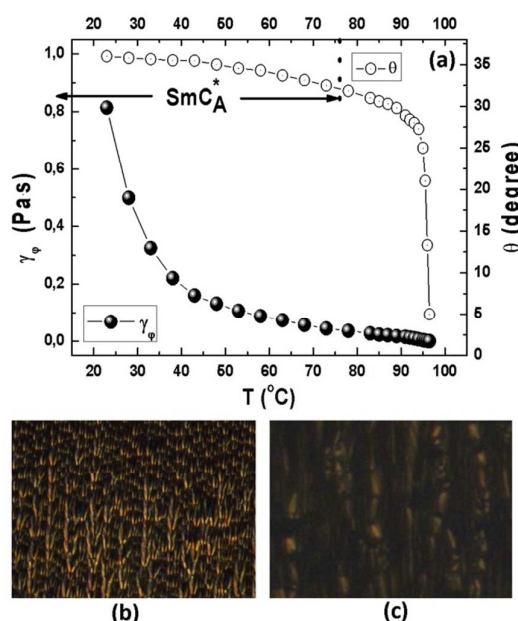


Fig. 6. (a) Temperature dependencies of the tilt angle (open circles) and rotational viscosity γ_ϕ (black circles) of the **AFLC-036** are presented; (b) and (c) are textures of planar aligned $1.7\mu\text{m}$ **AFLC-015** and **AFLC-036** layers placed between crossed polarizers, respectively. The size of the images is $200 \times 250\mu\text{m}$, the voltage is not applied.

Additionally, the alignment optical quality is better for the **AFLC-036**, in other words, the density of spatial inhomogeneities of the AFLC layer decreases for the highly concentrated AFLC, see Figs 6 (b) and 6 (c), which compare the optical quality of the **AFLC-015** and **AFLC-036**. The smaller p_0 of the **AFLC-036** is probably responsible for the better alignment quality.

Behaviour of the two parameters: (i) the principal optical axis of the helical structure (right insertion to Fig. 4) which deflects continuously and almost linearly by an angle $\Psi(E)$ up to $10 - 11^\circ$ and (ii) almost constant χ_G when $E \leq 0.8E_c$ (left insertion to Fig. 4), are similar to the well-known electro-optical DHF-effect in smectic-C* helical structure.⁵⁶⁻⁵⁸

Additional evidences for the similarity of electro-optical behaviour of AFLC cells for $E \leq E_c$ and the DHF-effect in smectic C* phase are given in Fig. 7 wherein, the characteristic relaxation times increase sharply in the close vicinity of E_c , but almost independent on applied electric field at $E \ll E_c$.

Thus, form the considerations based on above-mentioned facts it can be affirmed that the electro-optical behavior of the AFLC cells, for $E < E_c$ is similar to the deformed helix ferroelectric liquid crystals, and therefore, we can term it as the deformed helix antiferroelectric (DHAFLC) effect.

The applied stair waveform of the applied electric field E (see the inset Fig. 7) allows to measure the switching ON (τ_{on}) and switching OFF (τ_{off}) times, separately. In contrast to electro-optical effects in nematic liquid crystals (NLCs), where usually $\tau_{on} \ll \tau_{off}$ in the range of few milliseconds at the best, DHAFLC effect exhibits $\tau_{on} \gg \tau_{off}$ with at least 1-2 orders of magnitude faster than that of NLCs. The values of the switching times are $\tau_{on} \cong 400 \mu\text{s}$, and $\tau_{off} \cong 20 \mu\text{s}$ (Fig. 7).

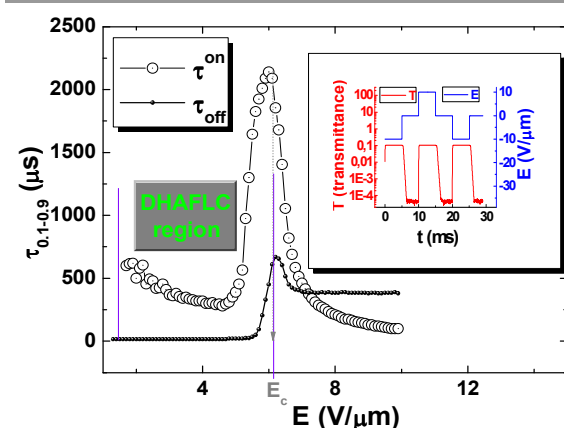


Fig. 7. (Color online). Dependencies of switching on (τ_{on}) and off (τ_{off}) times of AFLC-036 electro-optical response on applied electric field at temperature $T = 30^\circ\text{C}$, $\beta = 0$, wavelength $\lambda = 632.8 \text{ nm}$, and the applied voltage frequency $f = 100 \text{ Hz}$. The inset shows the electro-optical response of LC cell (the lower curve) from applied stair voltage.

At $\beta = \psi$ the electro-optical response time $\tau_{0.1-0.9}$ measured at applied square voltage and the T_{LT} value both are almost independent of temperature in a range $20^\circ\text{C} - 45^\circ\text{C}$ in DHAFLC mode, herewith $T_{LT} \approx 40\%$. Note, that $\tau_{0.1-0.9} \cong 65 - 70 \mu\text{s}$ under conditions mentioned above (Fig. 8).

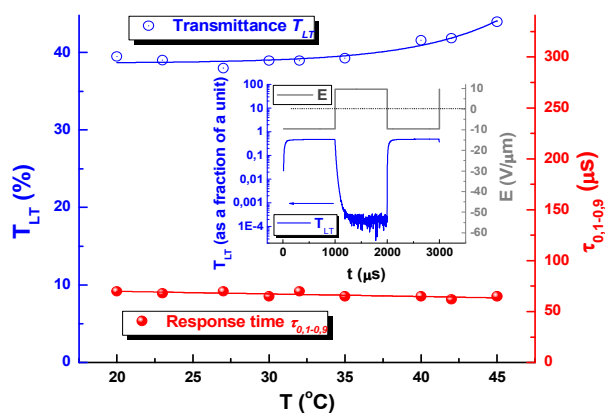


Fig. 8. (Color online). Temperature dependencies in DHAFLC mode of the electro-optical response time $\tau_{0.1-0.9}$ and light transmittance T_{LT} (compared with the transmittance of an empty cell placed between crossed polarizers) of $1.5 \mu\text{m}$ thick AFLC-036 layer placed between crossed polarizers at $\beta = \psi$, $f = 1 \text{ kHz}$, $\lambda = 632.8 \text{ nm}$. Applied square electric field tension is $E = 10 \text{ V}/\mu\text{m}$, see insert to Fig. 8.

In addition, the contrast ratio ($CR = T_{LTmax}/T_{LTmin}$) reaches 1000:1 with DHAFLC electro-optical effect (see insets of Fig. 7 and Fig. 8) that provides promising prerequisites for applications because of fast and stable operations in a broad temperature range. However, the light transmittance T_{LT} is limited to 40% and further research is required to improve it for the modern applications.

At $E > E_c$ the light transmittance of cells jumps up and tends to the saturation very fast, forming a typical electro-optical AFLC hysteresis loops at repolarization of the applied voltage, and the shape of the loops is highly dependent on the shape and frequency of the applied voltage, Fig. 9. As it is well-known fact that the characteristics of the deformed helix mode strongly depend on the frequency of the applied voltage,^{47,59} therefore, we have studied the dispersion parameters of hysteresis loop that is plotted in Fig. 9. Interestingly, the voltage coercivity measured at applied triangular voltage (V_c^{triang}) is always larger than that at applied stair voltage (V_c^{stair}), and frequency dispersions $V_c^{triang}(f)$ and $V_c^{stair}(f)$ are quite opposite Fig. 9(b). Moreover, the profile of $V_c^{triang}(f)$ dependency is exactly in the same as in the case of smectic C* phase because of viscous torque.^{59,60}

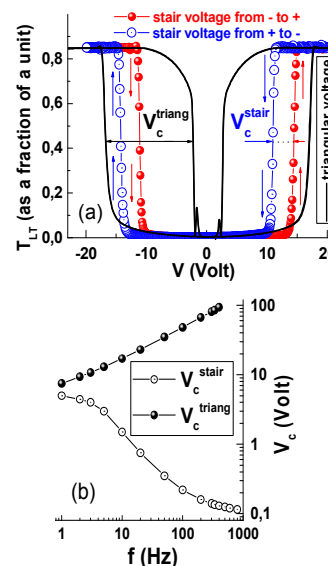


Fig. 9 (Color online): (a) AFLC-036 electro-optical hysteresis loops measured at continuous repolarization of triangular and stair applied voltage at $T = 50^\circ\text{C}$, $\beta = 0$, $\lambda = 632.8 \text{ nm}$, the AFLC layer thickness $1.5 \mu\text{m}$, and the applied voltage frequency $f = 5 \text{ Hz}$; (b) dispersion curves $V_c^{triang}(f)$ and $V_c^{stair}(f)$ measured at the same settings as given in the caption to Fig. 8 (a).

Whereas for $V_c^{stair}(f)$ reduces almost to zero as the frequency increases, see Fig. 9(b). Therefore, we designed a new driving signal with two frequency and magnitude that is capable of offering a hysteresis-free U-shaped electro-optical response (see Fig. 10), with simple adjusting the frequency of driving stair voltage

to $f > 100$ Hz, which is followed by Fig. 9(b). To the best of our knowledge, this is first experimental observation of the effect, which was predicted by Petrenko and J.W. Goodby in 2007.²⁹

The region from 0 to \pm threshold voltage at the plots of both hysteresis and hysteresis-free EOP response often referred to pre-transition or pre-threshold phenomena. Their physical essence is the DHAFLC mode, which is a first stage of the U-shape switching and its contribution to the light transmittance strongly depends on the waveform, the frequency of applied voltage (as seen from the comparison chart Fig. 9(a) and Fig. 10), and on the ψ angle. Thus, it is possible to choose either DHAFLC or U-shape effects by simple changes in the driving settings.

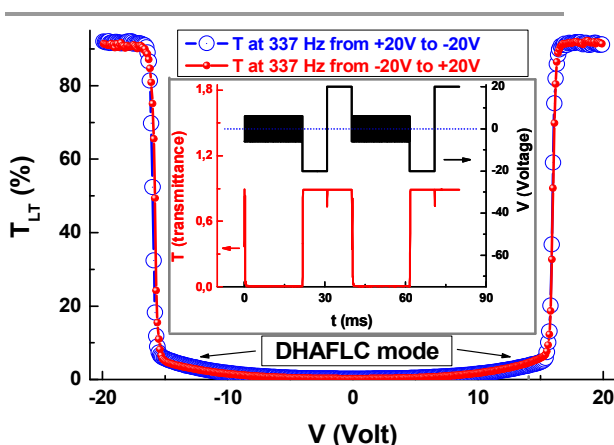


Fig. 10 (Color online). Hysteresis free U-shaped electro-optical response under applied stair voltage at $T = 60^\circ\text{C}$, $\beta = 0$, $\lambda = 632.8$ nm, the AFLC-036 layer thickness is $1.5\ \mu\text{m}$, and the applied voltage frequency $f = 337$ Hz. Insert shows electro-optical response of the cell (at the bottom) at applied dual frequency voltage (atop).

Furthermore, the said U-shape switching strongly depends on the pitch of the AFLCs. Plots for the U-shape switching at different pitch length, at different temperatures, have been plotted in Fig. 11. It is clear from the figure that the width and the threshold voltage increase at lower pitches. The dashed lines represent the threshold voltage for the AFLC with pitch ~ 140 nm that shows a clear shift at higher pitches. In other words, we can say that the threshold voltage decreases for the larger pitch. The threshold voltage is related with the E_c , which is $E_c \propto q_0^2$. The q_0 decreases with the increase in pitch, and therefore, the E_c and threshold voltage follow the same trend at the higher pitch.^{9,24} Hence, we can conclude that the V-shape switching of the AFLC with relatively larger pitch transforms to U-shape switching at smaller pitches.

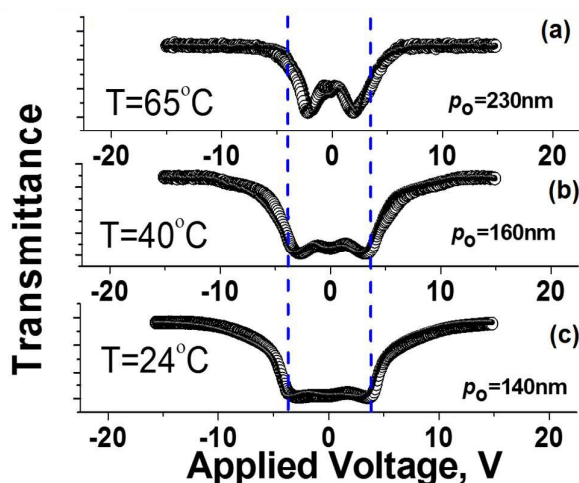


Fig. 11 Evolution of AFLC-015 electro-optical hysteresis loops depending on the helix pitch. Measurements have been carried out at continuous repolarization of stair applied voltage at $\beta = 0$, $\lambda = 632.8$ nm, and (a) $T = 65^\circ\text{C}$, $p_0 = 230$ nm; (b) $T = 40^\circ\text{C}$, $p_0 = 160$ nm; (c) $T = 24^\circ\text{C}$, $p_0 = 140$ nm.

Conclusions

In summary, use of two types of chiral dopants, i.e. esters of terphenyldicarboxylic acid containing in side wings chiral 2-trifluoromethylheptanol or trifluoromethylheptyllactate, induces unusual AFLC mesophase with nanoscale helix pitch in achiral smectic C host, biphenyl-pyrimidines. Two fast electro-optic effects in this mixture have been observed, first, DHAFLC and second, hysteresis free U-shape switching, which evolves from the V-shape as the pitch decreases (see Fig. 11).

The DHAFLC provides fast, almost temperature independent switching time ($< 65\ \mu\text{s}$ see Fig. 8) with the contrast ratio $\sim 1000:1$. The good alignment quality of ultra-short helix pitch (< 100 nm) manifests such a high contrast ratio.

The U-shaped electro-optical response of the proposed AFLCs is similar to NLCs, in shape, but two orders of magnitude faster. Both are hysteresis free, show a threshold, and therefore, the proposed AFLCs can be driven by the same driving waveforms as conventional LCDs and photonic dual frequency voltage devices.⁶¹

The DHAFLC mode, in comparison to the U-shape mode, offers higher contrast ratio that can be attributed to the optical axis (OA) modulation around the easy axis. For the dark state, the OA in the DHAFLC mode is parallel to the polarization azimuth of the impinging light, and therefore, the impinging light feels minimum retardation that results in a dark state with smaller transmittance and higher contrast ratio. On the other hand, U-shape AFLC mode reveals insufficient dark state, because it is a result of averaging of the OA

ARTICLE

Journal Name

deflection in the DHAFLC mode (see fig. 10), and therefore, it provides less contrast ratio (around 150:1) in comparison with the DHAFLC.

Acknowledgments

This work was supported by funds of State Key Laboratory on Advanced Displays and Optoelectronics Technologies, ECE Department, and grants under CERG 614410, CERG 612409, HKUST, Hong Kong, supported in part by Russian Foundation for Basic Research (RFBR) projects 16-29-14012, 16-02-00441, 15-59-32410, 15-02-08269, 15-32-20859 and of NAS of Ukraine (O112U002186, O114U000699). E.P. Pozhidaev thanks also RSCF (grant number 16-43-03010) for the financial support of experimental methods developing.

Notes and references

- H. Takezoe, E. Gorecka and M. Čepič, *Reviews of Modern Physics*, 2010, **82**, 897–937.
- M.B. Pandey, R. Dabrowski and R. Dhar, in Book: *Advanced Energy Materials*, ed. A. Tiwari and S. Valyukh, Publisher: WILEY–Scrivener, 2014, Pages 389–431.
- I. Dierking, *Materials*, 2014, **7**, 3568–3587
- M. B. Pandey, R. Verma and R. Dhar, *Isr. J. Chem.*, 2012, **52**, 895 – 907.
- P. Rudquist, *Liq. Cryst.*, 2013, **40**, 1678–1697.
- Y. Yamada, N. Yamamoto, K. Mori, K. Nakamura, T. Hagiwara, Y. Suzuki, I. Kawamura, H. Orihara and Y. Ishibashi, *Jpn. J. Appl. Phys.*, 1990, **29**, 1757–1764.
- N. Yamamoto, N. Koshoubu, K. Mori, K. Nakamura, and Y. Yamada, *Ferroelectrics*, 1993 **149**, 295–304.
- M. A. Geday, D. Poudereux, L. Crespo, J. M. Otón and X. Quintana, *Ferroelectrics*, 2016, **495**, 158–166.
- N. Olsson, I. Dahl, B. Helgee and L. Komitov, *Liq. Cryst.*, 2004, **31**, 1555–1568.
- P. Nayek, S. Ghosh, S. K. Kundu, S. K. Roy, T. P. Majumder, N. Bennis, J. M. Oton and R. Dabrowski, *J. Phys. D: Appl. Phys.*, 2009, **42**, 225504.
- B. Atorf, A. Hoischen, M.B. Ros, N. Gimeno, C. Tschierske, G. Dantlgraber and H. Kitzerow, *Appl. Phys. Lett.*, 2012, **100**, 223301.
- K. D'have, P. Rudquist, S. T. Lagerwall, H. Pauwels, W. Drzewinski and R. Dabrowski, *Appl. Phys. Lett.*, 2000, **76**, 3528–3530.
- S.T. Lagerwall, A. Dahlgren, P. Jägemalm, P. Rudquist, K. D'have, H. Pauwels, R. Dabrowski and W. Drzewinski, *Adv. Funct. Mater.*, 2001, **11**, 87–94.
- J. M. Oton, X. Quintana, P.L. Castillo, A. Lara, V. Urruchi and N. Bennis, *Opto–Electron. Rev.*, 2004, **12**, 263–269.
- N. Wakita, T. Uemoda and H. Ohnishi, *Ferroelectrics*, 1993, **149**, 229–238.
- P. Rudquist, D. Elfstrom, S. T. Lagerwall and R. Dabrowski, *Ferroelectrics* **2006**, 344, 177–188.
- J. Strauss and H.–S. Kitzerow, *Appl. Phys. Lett.*, 1996, **69**, 725–727.
- V. Prasad, S.–W. Kang and S. Kumar, *J. Mater. Chem.*, 2003, **13**, 1259–1264.
- W. Rejmer, M. Zurowska, R. Dabrowski, K. Czuprynski, Z. Raszewski and W. Piecek, *Mol. Cryst. Liq. Cryst.*, 2009, **509**, 195–205.
- A. Mishra, M. Zurowska, R. Dabrowski and R. Dhar, *Phase Transitions*, 2014, **87**, 746–757.
- M. Czerwiński and M. Tykarska, *Liq.Cryst.*, 2014, **41(6)**, 850–860.
- M. Tykarska and M. Czerwiński, *Liq.Cryst.*, 2016, **46(4)**, 462–472.
- J. M. Otón, J. M. S. Pena, X. Quintana, J. L. Gayo and V. Urruchi, *Appl. Phys. Lett.*, 2001, **78**, 2422–2424.
- A. K. Srivastava, V. G. Chigrinov and H. S. Kwok, *J. Soc. Inf. Disp.*, 2015, **23**, 253–272.
- M. Hird, J. W. Goodby, P. Hindmarsh, R. A. Lewis and K. J. Toyne, *Ferroelectrics*, 2002, **276**, 219–237.
- V. Vill, G. Peters, S. Thiemann and Z. Galewski, *LiqCryst Database*, Ver. 5.0.28, LCI Publisher GmbH.
- A. Eremin and A. J'akli, *Soft Matter*, 2013, **9**, 615–637.
- J. W. Goodby, J. S. Patel and E. Chin, *J. Mater. Chem.*, 1992, **2**, 197–207.
- A. Petrenko and J.W. Goodby, *J. Mater. Chem.*, 2007, **17**, 766–782.
- P. Lehmann, W. K. Robinson and H. J. Coles, *Mol. Cryst. Liq. Cryst.*, 1998, **328**, 229–236.
- M. Zurowska, R. Dąbrowski, J. Dziaduszek, K. Skrzypek, M. Filipowicz, W. Rejmer, K. Czupryński, N. Bennis and J. M. Otón, *J. Mater. Chem.*, 2011, **21**, 2144–2153.
- W. K. Robinson, P. Lehmann and H. J. Coles, *Mol. Cryst. Liq. Cryst.*, 1998, **328**, 221–228.
- Y. Aoki and H. Nohira, *Ferroelectrics*, 1996, **178**, 213–220
- A. Z. Rabinovich, M. V. Loseva, N. I. Chernova, E. P. Pozhidaev, O. S. Petrachevich and J. S. Narkevich, *Liq. Cryst.*, 1989, **6**, 533–543.
- E. P. Pozhidaev, S. I. Torgova, V. E. Molkin, M. V. Minchenko, V. V. Vashchenko, A. I. Krivoshey and A. Strigazzi, *Mol. Cryst. Liq. Cryst.*, 2009, **509**, 1042–1050.
- E. P. Pozhidaev, A. D. Kiselev, A. K. Srivastava, V. G. Chigrinov, H. S. Kwok and M. Minchenko, *Phys. Rev. E*, 2013, **87**, 052502.
- E. P. Pozhidaev, A. K. Srivastava, A. D. Kiselev, V. G. Chigrinov, V. V. Vashchenko, A. I. Krivoshey, M. V. Minchenko and H. S. Kwok, *Opt. Lett.*, 2014, **39**, 2900–2903.
- M.V. Kumar, S. K. Prasad, D. S. S. Rao, E. P. Pozhidaev, *Phase Transitions*, 2013, **86**, 323 – 338.
- M. Loseva, N. Chernova, A. Rabinovich, E. Pozhidaev, Yu. Narkevich, O. Petrashevich, E. Kazachkov, N. Korotkova, M. Schadt and R. Buchecker, *Ferroelectrics*, 1991, **114**, 357–77.
- E. V. Popova, E. I. Kopeychenko, A. I. Krivoshey, V. V. Vashchenko and A. P. Fedoryako, *Phys. Rev. E.*, 2012, **86**, 031705.
- K. Terashima, M. Ichihashi, F. Takeshita, M. Kikuchi and K. Furukawa, EP 0293763 A2, Chisso Corporation, Jun 01, 1987.
- P. V. Ramachandran, A. V. Teodorovic, B. Gong and H. C. Brown, *Tetrahedron: Asymmetry*, 1994, **5**, 1075–1086.
- T. Yonezawa, Y. Sakamoto, K. Nogawa, T. Yamazaki and T. Kitazume, *Chem. Lett.* 1996, **25**, 855–856.
- V. Mikhailenko, D. Yedamenko, G. Vlasenko, A. Krivoshey and V. Vashchenko, *Tetrahedron Lett.*, 2015, **56**, 5956–5959.

- 45 B. Neises and W. Steglich, *Angew. Chem. Int. Ed.*, 1978, **17**, 522–524.
- 46 V. Vashchenko, A. Krivoshey, I. Knyazeva, A. Petrenko and J. W. Goodby, *Tetrahedron Lett.*, 2008, **49**, 1445–1449.
- 47 E. Pozhidaev, V. Chigrinov, A. Murauski, V. Molkin, D. Tao and H. S. Kwok, *J. Soc. Inf. Disp.*, 2012, **20**, 273–278.
- 48 A. D. Kiselev, E. P. Pozhidaev, V. G. Chigrinov and H. S. Kwok, *Phys. Rev. E*, 2011, **83**, 031703.
- 49 E. P. Pozhidaev, M. A. Osipov, V. G. Chigrinov, V. A. Baikalov, L. M. Blinov and L. A. Beresnev, *J. Exp. Theor. Phys.*, 1988, **94**, 283–287.
- 50 M. I. Barnik, V. A. Baikalov, V. G. Chigrinov and E. P. Pozhidaev, *Mol. Cryst. Liq. Cryst.*, 1987, **143**, 101–112.
- 51 V. Panov, J. K. Vij and N. M. Shtykov, *Liq. Cryst.*, 2001, **28**, 615–620.
- 52 D. W. Berreman, *Mol. Cryst. Liq. Cryst.*, 1973, **22**, 175–184.
- 53 K. Hori, *Mol. Cryst. Liq. Cryst.*, 1982, **82**, 13–17.
- 54 K. L. Sandhya, A. D. L. Chandani, A. Fukuda, J. Vij, A. V. Emelyanenko and K. Ishikawa, *Phys. Rev. E*, 2013, **87**, 012502.
- 55 A. V. Kaznacheev and E. P. Pozhidaev, *JETPH*, 2012, **114**, 1043–1051.
- 56 A. Strigazzi, S. Torgova, E. Pozhidaev, A. S. Gliozzi, *Liq. Cryst.*, 2016, **43**, 153–161.
- 57 L. A. Beresnev, V. G. Chigrinov, D. I. Dergachev, E. P. Pozhidaev, J. Funfshilling and M. Schadt, *Liq. Cryst.*, 1989, **5**, 1171–1177.
- 58 E. Pozhidaev, S. Torgova, M. Minchenko, C. A. R. Yednak, A. Strigazzi and E. Miraldi, *Liq. Cryst.*, 2010, **37**, 1067–1081.
- 59 C. Reynaerts and A. de Vos, *Ferroelectrics*, 1991, **113**, 439–452.
- 60 A. D. Kiselev, V. G. Chigrinov and E. P. Pozhidaev, *Phys. Rev. E*, 2007, **75**, 061706.
- 61 Y. Yin, S. V. Shiyonovskii and O. D. Lavrentovich, *Phys. Rev. Letts.*, 2007, **98**, 097801.